



Article

Reversible Data Hiding in JPEG Images Using Quantized DC

Suah Kim ^{1,*} , Fangjun Huang ² and Hyoung Joong Kim ¹ ¹ School of Information Security, Korea University, Seoul 02821, Korea² School of Data and Computer Science, Sun Yat-sen University, Guangzhou 510006, China

* Correspondence: suahnkim@gmail.com

Received: 7 July 2019; Accepted: 23 August 2019; Published: 26 August 2019



Abstract: Reversible data hiding in JPEG images has become an important topic due to the prevalence and overwhelming support of the JPEG image format these days. Much of the existing work focuses on embedding using AC (quantized alternating current coefficients) to maximize the embedding capacity while minimizing the distortion and the file size increase. Traditionally, DC (quantized direct current coefficients) are not used for embedding, due to the assumption that the embedding in DCs cause more distortion than embedding in ACs. However, for data analytic which extracts fine details as a feature, distortion in ACs is not acceptable, because they represent the fine details of the image. In this paper, we propose a novel reversible data hiding method which efficiently embeds in the DC. The propose method uses a novel DC prediction method to decrease the entropy of the prediction error histogram. The embedded image has higher PSNR, embedding capacity, and smaller file size increase. Furthermore, proposed method preserves all the fine details of the image.

Keywords: reversible data hiding; JPEG; DCT coefficients; DC coefficients; entropy

1. Introduction

JPEG image file format has proved its dominance year after year. Even with the new image standard that supports higher efficiency and compression, it still comes as a default image standard for storing images in smartphones and computers. With unparalleled support for it in variety of devices and software, reversible data hiding JPEG image has become an important topic.

Reversible data hiding is an interoperable data hiding method, which preserves the original file format and has ability to recover the original image from the embedded or watermarked image. But it is different than robust watermarking scheme such as one proposed by Liu et al. [1], which focus on recovery of the embedded message under image processing attacks.

The embedded image should be as close as possible to the original image and the PSNR value is measured against different payload size to compare the performance of the data hiding capability.

Much of the research focused on reversible data hiding is in pixel domain. They are based on lossless compression [2–6], difference expansion [7–13], or histogram shifting [7,14–39]. A recent advances [19,20,39,40] use two dimensional histogram shifting to achieve higher embedding capacity and lower distortion. Furthermore, a new research field using reversible data hiding, which focuses on adapting reversible data hiding technique as an image enhancement technique, has emerged [41–48]. In particular, some [41,42] proposed using reversible data hiding technique for automatic image enhancement and use the reversibility as an advantage to save storage space. Reversible data hiding can be also used before image encryption [49,50] to hide additional data or to obscure the size of the image in a reversible way.

On the other hand, reversible data hiding in JPEG has not been extensively researched. There are three main approaches: the first approach modifies the quantization table to artificially increase

the quantized DCT coefficients and embed [51,52]. Although this approach has high embedding capacity, the file size increase is much larger than the obtained embedding capacity. The second approach modifies the Huffman table [53–55]. Although this approach preserves the file size, the embedding capacity is quite limited. The third approach modifies the quantized DCT coefficients for embedding [56–64]. It is most logical approach given that it directly modifies the visual features without modifying other image parameters (such as Huffman table and quantization table).

The proposed method is a third approach, which uses a prediction scheme for quantized DC coefficients. The proposed prediction provide improved accuracy, which decreases the entropy of the quantized DC prediction error histogram to have large embedding capacity with lower distortion. Furthermore, proposed method only modifies the quantized DC values.

The main goal of reversible data hiding in JPEG is to achieve high PSNR without causing much change in the file size, but there are specific cases where quantized AC coefficient preservation is required and is more important than achieving high PSNR. Consider a case where embedded images are used for image data analysis for searching specific patterns or an object. Image data analysis rely on feature extraction of fine image details, which the AC coefficients represent (see Figure 1 for an example). Without the AC coefficient preservation, data analytic may not perform as well.

The proposed method provides a novel reversible data hiding technique which can embed in the quantized DC coefficients. Unlike existing work, all the fine details are preserved since none of the AC coefficients are modified.

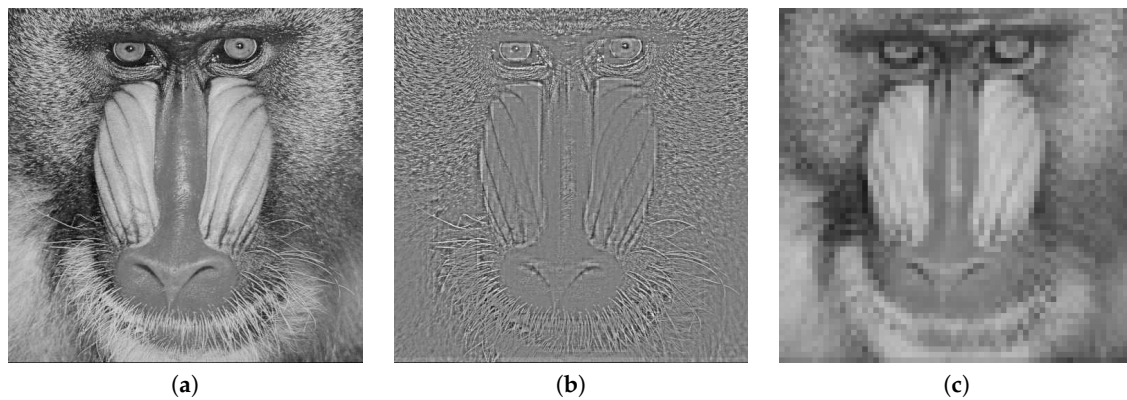


Figure 1. Reconstructed JPEG image of Baboon using different sets of quantized DCT coefficients. Quantized DC coefficients preserves the overall intensity, whereas quantized AC coefficients preserve the fine details of the image, making them less ideal for embedding for cases where fine details matter. (a) all quantized DCT coefficients; (b) quantized AC coefficients; (c) quantized DC coefficients.

2. Brief Introduction to JPEG Baseline Encoding and Decoding

This section briefly describes the JPEG baseline encoding and decoding steps to aid with understanding of the proposed method. JPEG is a block based lossy compression technique which transforms 8 by 8 pixel blocks into to 8 by 8 quantized DCT coefficient blocks. The transformation consists of normalization by subtracting 128 from each of the pixels, discrete cosine transform (DCT), division by the quantization table, which is usually scaled using a scaling factor called quantization factor (QF) to control the effect of the compression and the image quality, and rounding is applied to make the values integral.

DCT is defined as following:

$$DCT_{u,v} = \frac{\alpha(u)\alpha(v)}{4} \sum_{i=0}^7 \sum_{j=0}^7 p_{i,j} \cos\left[\frac{(2i+1)u\pi}{16}\right] \cos\left[\frac{(2j+1)v\pi}{16}\right] \quad (1)$$

where

$$\alpha(u) = \begin{cases} \frac{1}{\sqrt{2}} & \text{if } u = 0 \\ 1 & \text{if } else \end{cases} \quad (2)$$

where $p_{i,j}$ represents the pixel value at position (i,j) and $DCT_{u,v}$ represents the DCT value at position (u,v) .

Once the quantized DCT coefficients are obtained, they are compressed losslessly. Quantized DCT coefficients consist of quantized DC and quantized AC coefficients. The quantized DC coefficient is the first DCT coefficient value and represents a form of a mean pixel value. The quantized AC coefficients are the rest of the DCT coefficients and represents the fine details of the pixel block. Differential pulse code modulation (DPCM), where the difference between two consecutive values is encoded, is used to compress the quantized DC coefficients in two adjacent blocks. Then, DPCM values are losslessly compressed using a variant of Huffman coding. For the quantized AC coefficients, run length coding is applied, and then encoded using a variant of Huffman coding.

To reconstruct the pixels from the quantized DCT coefficients, the quantized DCT coefficients are multiplied with the quantization table and then, inverse DCT is applied. Then, 128 is added to each value to undo the normalization, and finally, rounding function is used to make the result integral. More information about JPEG encoding and decoding can be found in the ISO document [65].

From here on, the quantized DCT coefficients (including quantized AC and DC coefficients) are denoted by bold font: DCT, AC, and DC.

3. Proposed Method

The proposed method uses a reversible data hiding technique called histogram shifting, where the performance is highly dependent on the prediction accuracy. The embedding and distortion of histogram shifting is relative to the prediction error; smaller prediction errors mean higher embedding capacity with lower distortion.

Previous work does not utilize advanced prediction in JPEG reversible data hiding. This is because of the assumption that the prediction in the DCT domain is difficult and is not worth the effort. Although the assumption is true in general, it is not true for all DCT. The first DCT in the DCT transformed block, also referred as the DC, represents the $\frac{8}{Q_1} \times$ mean normalized pixel values in the block, where Q_1 is the quantization table entry for quantizing the DC value. The proposed method builds upon this idea to propose a DC prediction method, which will increase the embedding capacity and decrease the distortion.

Figure 2 shows histograms of image Lena (QF = 50). The histogram of DC does not have a peak and has the largest entropy, the histogram of differential pulse code modulated (DPCM) DC is better for histogram shifting than DC histogram, because it has a high peak around 0 and lower entropy, and finally, the histogram of proposed DC prediction error histogram has the highest peak and the smallest entropy, making it ideal for histogram shifting.

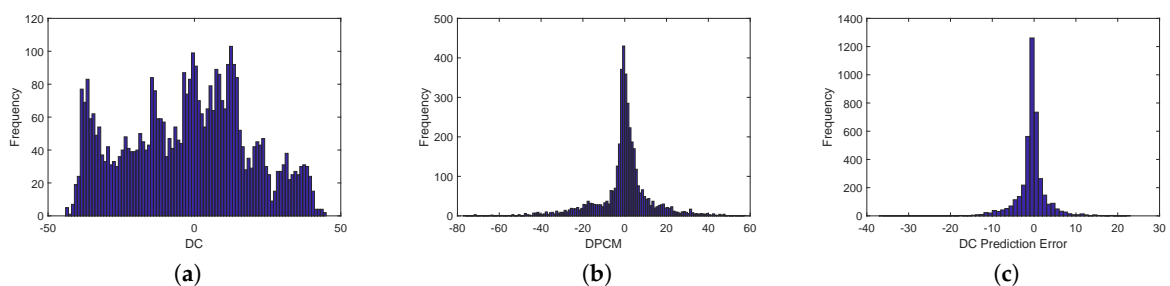


Figure 2. Comparison of different histograms. The proposed DC prediction error histogram has the highest peak and the smallest entropy. (a) DC histogram; (b) DPCM DC histogram; (c) DC prediction error histogram.

The next subsections describe DC prediction method, embedding method, and extraction method.

3.1. DC Prediction

Unlike the prediction in image compression, where only decoded blocks can be used for prediction, prediction in reversible data hiding can utilize all blocks which are not used for embedding. In other words, we can divide the blocks into two non-overlapping alternating sets, “white” and “black” sets, and embed them one at a time to facilitate more accurate prediction (see Figure 3). Without loss of generality, the white set is embedded first then the black.

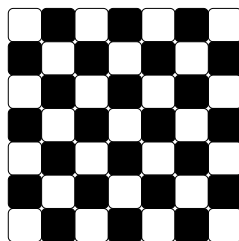


Figure 3. DCT blocks are divided in two alternating sets of white and black blocks.

Before explaining the proposed prediction, we define ‘ T ’ or ‘target block’ as the block which we want to predict the DC of. Furthermore, the superscript AC is used to denote that the block is reconstructed only using the AC component.

Then, let T^{AC} denote the partially reconstructed pixel target block using only the AC from the target block (DC value is set as 0). Then, because DCT is a linear function, T can be approximately decomposed as following:

$$T \approx T^{AC} + DC \times \frac{Q_1}{8} \quad (3)$$

where Q_1 is the quantization value which divided the DC coefficient to get DC, and $DC \times \frac{Q_1}{8}$ represents the effect of the inverse DCT on DC.

The proposed prediction uses the neighboring blocks and the partially reconstructed blocks using only the AC component. The neighboring DCT blocks are first transformed to pixel blocks of “North”, “East”, “South”, and “West”.

Figure 4 shows graphical view of the division. The red area represents the parts of neighbors which are closest to the target block, and the yellow area represents the parts of the target block which are closest to the neighboring blocks. Using this setup, we assume that the pixels from the neighboring blocks and the pixels from the target block, which are exactly one position away from each other, should be similarly valued:

$$\text{Pixel}_{\text{red}} \approx \text{Pixel}_{\text{yellow}} \quad (4)$$

where $\text{Pixel}_{\text{red}}$, the pixel from the neighboring block, and $\text{Pixel}_{\text{yellow}}$, the pixel from the target block, are exactly one position away from each other. In Figure 5, W_8 is exactly one position away from T_1 , but is two positions away from N_{57} and T_9 .

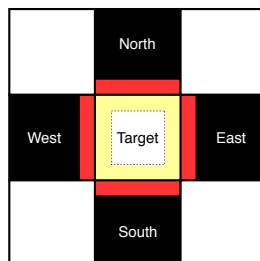


Figure 4. Example of the context used for prediction. DC is predicted using four direct neighboring black blocks and the AC of the target block.

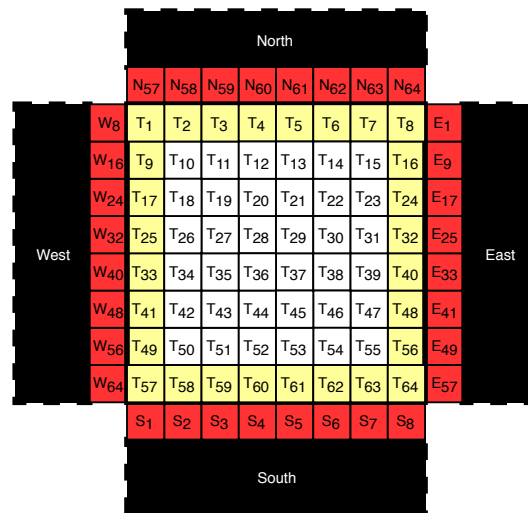


Figure 5. Contexts used for predicting DC. The neighboring pixel values from already decoded blocks (North, West, South, and East), and partially reconstructed target block T^{AC} is used to improve the prediction accuracy.

Combining Equations (3) and (4), we get following approximation:

$$\text{Pixel}_{\text{red}} \approx \text{Pixel}_{\text{yellow}}^{AC} + \text{DC} \times \frac{Q_1}{8} \quad (5)$$

By rearranging the above equation, $\hat{\text{DC}}$, the predicted value of DC is:

$$\hat{\text{DC}} = \left[\frac{8}{Q_1} \times (\text{Pixel}_{\text{red}} - \text{Pixel}_{\text{yellow}}^{AC}) \right] \quad (6)$$

where $[\cdot]$ is the rounding function.

Finally, since there are multiple $\text{Pixel}_{\text{red}}$ and $\text{Pixel}_{\text{yellow}}^{AC}$, the mean is used as an estimator to evaluate $\hat{\text{DC}}$:

$$\hat{\text{DC}} = \left[\frac{8}{Q_1} \times \frac{\sum_{\text{neighbor}} (\text{Pixel}_{\text{red}} - \text{Pixel}_{\text{yellow}}^{AC})}{\# \text{ of neighbors}} \right] \quad (7)$$

$$= \left[\frac{8}{Q_1} \times \frac{\sum_{\text{North, East, South, West}} (\text{Pixel}_{\text{red}} - \text{Pixel}_{\text{yellow}}^{AC})}{32} \right] \quad (8)$$

$$= \left[\frac{8}{Q_1} \times \frac{\sum_{n=1}^8 (N_{56+n} - T_n^{AC}) + (E_{8n-7} - T_{8n}^{AC}) + (S_n - T_{n+56}^{AC}) + (W_{8n} - T_{8n-7}^{AC})}{32} \right] \quad (9)$$

3.2. Embedding

Histogram shifting technique is used to embed in the prediction error values $(\text{DC} - \hat{\text{DC}})$. Embedded DC is denoted by DC' , and is obtained using following equation:

$$\text{DC}' = \begin{cases} \text{DC} - b & \text{if } \text{DC} - \hat{\text{DC}} = -1 \\ \text{DC} + b & \text{if } \text{DC} - \hat{\text{DC}} = 0 \\ \text{DC} - 1 & \text{if } \text{DC} - \hat{\text{DC}} < -1 \\ \text{DC} + 1 & \text{if } \text{DC} - \hat{\text{DC}} > 0 \\ \text{DC} & \text{else} \end{cases} \quad (10)$$

$b \in \{0, 1\}$ is the payload bit.

The histogram shifting technique shifts **DC** with prediction errors less than -1 by -1 , so that **DCs** valued -1 can be embedded using coefficients valued -1 and -2 : the coefficient valued -1 is modified to -2 if the payload bit is “1”, and left as -1 if the payload bit is “0”. Similar logic applies to **DC** with prediction error greater than 0. Since the histogram shifting is applied such that none are overlapping, it can be reversed. The next subsection discusses the extraction of the payload and the recovery of the original **DC**.

3.3. Extraction and Recovery

The extraction of the payload and the recovery of the original **DC** are trivial.

$$b = \begin{cases} 0 & \text{if } \mathbf{DC}' = -1 \\ 0 & \text{if } \mathbf{DC}' = 0 \\ 1 & \text{if } \mathbf{DC}' = -2 \\ 1 & \text{if } \mathbf{DC}' = 1 \end{cases} \quad (11)$$

$$\mathbf{DC} = \begin{cases} \mathbf{DC}' + 1 & \text{if } \mathbf{DC}' - \hat{\mathbf{DC}} < -1 \\ \mathbf{DC}' - 1 & \text{if } \mathbf{DC}' - \hat{\mathbf{DC}} > 0 \\ \mathbf{DC}' & \text{else} \end{cases} \quad (12)$$

3.4. Block Selection

Block selection is important for cases where full embedding capacity is not utilized. In order to have the smallest impact on the PSNR, blocks are sorted by their smoothness and blocks are embedded sequentially only until all the payload is embedded.

To ensure that the smoothest blocks are embedded first, block selection algorithm proposed by Huang et al. [62] is used. In their algorithm, number of zero **DCT** coefficients are used as a smoothness measure to sort the blocks. The assumption here is that the **DCT** blocks with more zero **DCT** coefficients will have less details and thus be smoother.

In the proposed method, zero **DC** coefficients are not used to measure the smoothness and only the zero **AC** coefficients are used to measure the smoothness. **DC** coefficients are not used, because they may change after embedding.

4. Encoder and Decoder

This section summarizes the encoding and decoding method of the proposed reversible data hiding scheme. Each subsection will describe the implementation steps and include minor implementation details to aid with understanding.

4.1. Encoder

1. Extract the **DCT** blocks from JPEG image.
2. Divide the blocks into white and black set.
3. Use block selection method to sort the white set of **DC**.
4. Predict the white set of **DC** and embed half of the payload.
5. Use block selection method to sort the black set of **DC**.
6. Predict the black set of **DC** and embed the rest of the payload including the payload length, which is appended in front of the rest of the payload. (Prediction uses the embedded **DC'** from step 4.)

4.2. Decoder

1. Extract the embedded **DCT** blocks from JPEG image.
2. Divide the blocks into white and black set.

3. Use block selection method to sort the black set of \mathbf{DC}' .
4. Predict the black set of \mathbf{DC}' , extract the payload length and the half of the payload, and recover the original \mathbf{DC} for the black set.
5. Use block selection method to sort the white set of \mathbf{DC} .
6. Predict the white set of \mathbf{DC}' , extract the first half of the payload, and recover the original \mathbf{DC} for the white set. (Prediction uses the original \mathbf{DC} recovered from step 4.)

5. Experiment

The performance of the proposed method is verified using PSNR (between the original JPEG and the embedded JPEG) and the file size gain (due to embedding) comparison. However, there are no existing work that focus only on embedding in \mathbf{DC} . Thus, a variant of Huang et al.'s method [62], which is the state of the art algorithm in terms of PSNR and file size gain, is compared with the proposed method.

Methods such as Wang et al. [66], Xuan et al. [58], and Sakai et al. [59] are not compared here, as Huang et al.'s method produces images with higher PSNR with respect to the file size gain. See reference [62] for more detailed comparison. Improved version of Huang et al.'s work by Wedaj et al. [64] is not compared here either, since their method is the optimization of choosing multiple AC coefficients per block for embedding (the proposed method uses single DCT for embedding, comparison would not be fair). Without the optimization, Wedaj et al.'s method is the same as Huang et al.'s.

For fair comparison, a variant of Huang et al.'s method is used for the comparison. Although the original method only embeds in \mathbf{AC} , it can be modified to embed in DPCM of \mathbf{DC} with values 0 and -1 . When embedded this way, Huang et al.'s method also preserves the \mathbf{AC} coefficients just like the proposed method.

Quantization factor (QF) values of 50 and 80 are chosen for comparison. QF = 50 based quantization table is the recommended base quantization table written in the standard document, which is scaled to obtain other quantization table, making it a good benchmark for test against. QF = 80 based quantization table is the table which is known to achieve good compression to visual degradation ratio.

The code for the proposed method will be available at <https://github.com/suahnkim/jpegrwdc> (accessed on 23 August 2019).

6. Discussion and Analysis

For testing, two image sets are chosen. To see the comparison using the well-known images, the first image set includes 6 images, "Lena", "Boat", "Barbara", "Baboon", "Peppers", and "F16" from USC-SIPI image data set (<http://sipi.usc.edu/database/>) (accessed on 23 August 2019). The original bmp images are JPEG compressed to the size of 512×512 . These images are chosen specifically for comparing specific unique features. For more general comparison, the second image set includes 1000 images from Alaska image data set (<https://alaska.utt.fr/>) (accessed on 23 August 2019). The original raw .cr2 images are JPEG compressed to the size of 432×648 .

6.1. Comparison Using USC-SIPI Image Data Set

In this section, USC-SIPI database is used to compare for specific features. PSNR value relative to the size of the embedded payload and the file size gain due to embedding the payload are compared.

6.1.1. PSNR Comparison Using USC-SIPI Image Data Set

Figure 6 summarizes the PSNR comparison: "Huang QF = 50" represents the result when Huang et al.'s method is used to embed in the QF = 50 image, and "Huang QF = 80" represents the result when Huang et al.'s method is used to embed in the QF = 80 image. Same notation applies for the proposed method.

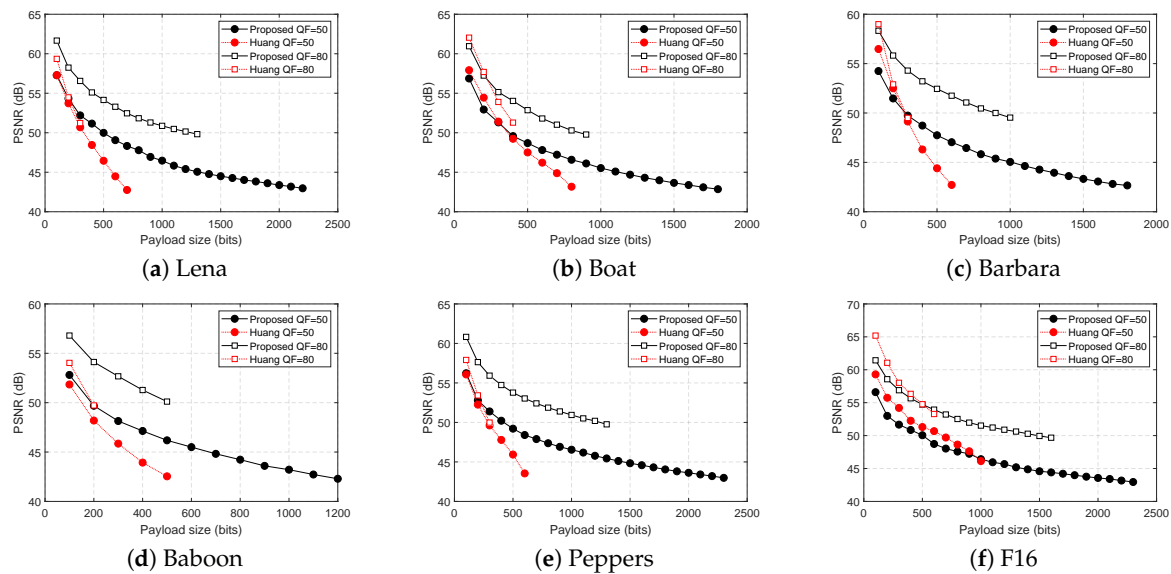


Figure 6. PSNR comparison for different payload sizes.

Both methods preserve the AC coefficients as required, but the proposed method has higher PSNR and embedding capacity for almost all images except the image F16. The proposed method consistently can embed more than 15% of the total blocks, and for few of the images it can embed more than 50%, whereas Huang et al.'s method can only embed between 5% and 25%.

Upon close inspection on the prediction error histograms of F16, DPCM is a better predictor for first few sets of payload. This is not surprising because F16 is a very smooth image. However, this is a single outlier, and the proposed method's prediction is generally better and more consistently accurate than DPCM. More importantly, the proposed method can consistently embed more than Huang et al.'s.

6.1.2. File Size Gain Comparison Using USC-SIPI Image Data Set

File size gain due to embedding is an important measure in JPEG reversible data hiding. JPEG is designed to offer good compression capability with respect to the image quality, thus reversible data hiding should not increase the file size significantly. Ideally, the file size gain due to embedding should be smaller than the embedded payload size.

Figure 7 summarizes the comparison result for the file size gain. The file size gain is measured against the size of the embedded payload. To clearly see whether the embedding caused more file size gain than the size of the payload, a straight line through the middle is drawn. The proposed method consistently has smaller file size gain than Huang et al.'s for both QFs. Furthermore, it has smaller file size gain than the size of the payload for all cases. This implies that when proposed method is used for embedding, it will not increase the file size more than the size of the payload.

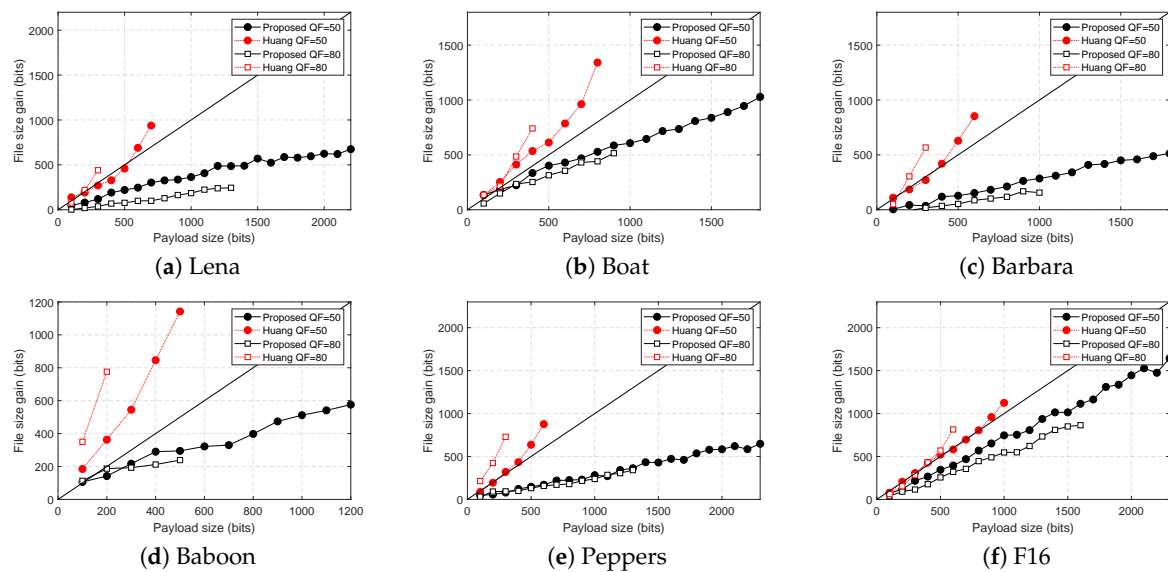


Figure 7. File size comparison for different payload sizes. The black straight line in the middle represents the equality for the file size gain and payload sizes.

6.2. Comparison Using Alaska Image Data Set

In this section, performance comparison using Alaska image data set is summarized. Unlike the earlier comparison which compared specific images, the comparison here uses 1000 images to compare using more robust statistical results. For the comparison, PSNR gain, file size difference, and payload gain are compared.

Applying reversible data hiding in 1000 JPEG images produces many data points: each image has different maximum payload size, and each payload size gives different PSNR value and file size. Fair comparison is done by only comparing the results for the same image and same payload size.

6.2.1. PSNR Gain Comparison Using Alaska Image Data Set

PSNR gain measures the difference between the PSNR values of the embedded image using proposed method and Huang et al.'s. Figure 8a summarizes the result for the average PSNR difference for different payload sizes. The results are all positive, meaning that the proposed method produced embedded images with higher PSNR than Huang et al.'s in average.

6.2.2. File Size Difference Comparison Using Alaska Image Data Set

File size difference is the difference between the file sizes of the embedded image using the proposed method and Huang et al.'s. This is used to show that the proposed method produces embedded image with smaller file size. Figure 8b summarizes the result for the average file size difference when different payload sizes are embedded. The negative value means that the file size of the embedded image using the proposed method is smaller than Huang et al.'s, and opposite for the positive values. Clearly, the proposed method has smaller file size gain due to embedding in average.

6.2.3. Payload Gain Comparison Using Alaska Image Data Set

Payload gain is the difference between the maximum payload sizes of the Huang et al.'s and the proposed method. This is compared to show the difference in maximum embeddable payload size for each image. Figure 8c summarizes the result. Positive payload gain means that the proposed method can embed that much more, and opposite for the negative values. For all cases except one, the proposed method embeds more than Huang et al.'s for both QF = 50 and QF = 80. In average, proposed method can embed 1570 bits more for QF = 50, and 1163 bits more for QF = 80.

Furthermore, Huang et al.'s could not embed any payload for 24 out of 1000 images for $QF = 50$, and 35 out of 1000 images for $QF = 80$, whereas the proposed method manages to embed in all images. The result clearly shows that the proposed method can embed far more than Huang et al.'s.

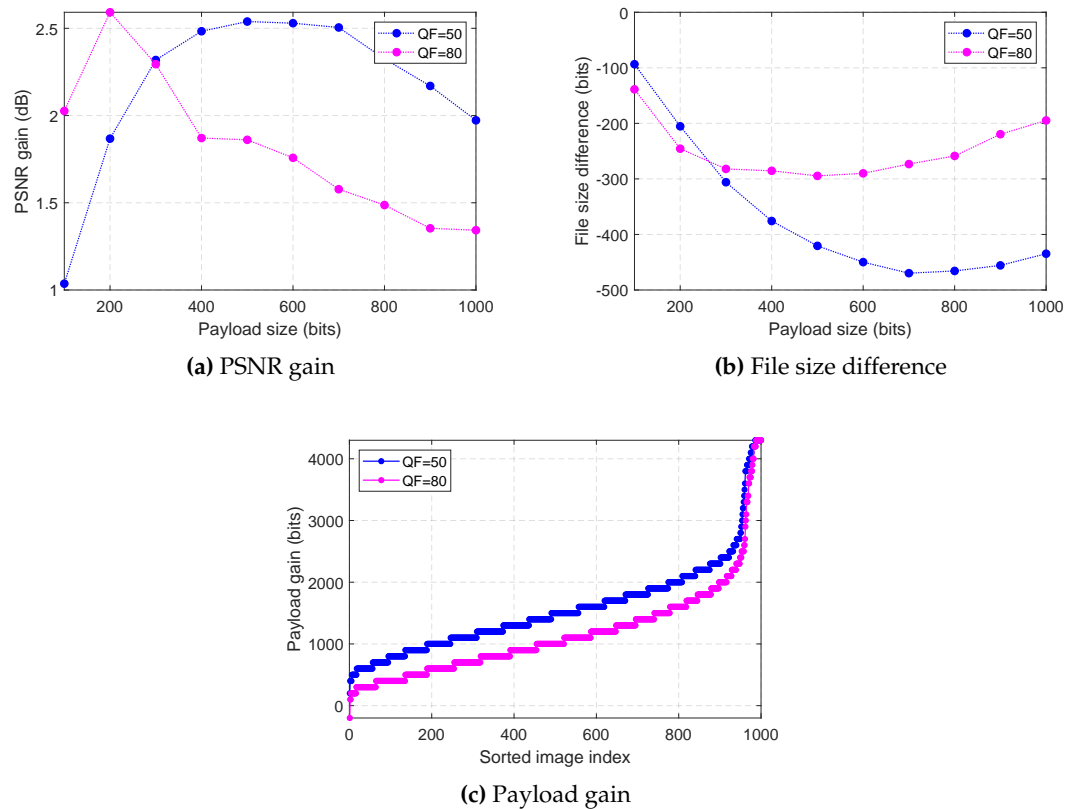


Figure 8. Extended comparison using Alaska image data set.

7. Effectiveness of the Block Sorting Algorithm in General

In this section, we analyze and discuss the effect of the block sorting algorithm with respect to the prediction error histogram resulting from the proposed method. In reversible data hiding, block sorting algorithm is used to control the rate of embedding such that the smallest number of DC can be used for embedding to minimize the impact on the PSNR.

In the proposed method, only prediction error valued 0 and -1 are used for embedding. However, it can be modified to embed in other prediction error values, such as 1 and -1 , or even multiple pairs. Naturally, it is not possible to measure the performance of the block sorting algorithm with respect to all possible modifications.

Instead of measuring the performance for all possible modification, we proposed analyzing the prediction error histogram using the entropy to measure the general effectiveness of the block sorting algorithm. Ideally, block sorting algorithm should sort the blocks such that blocks which are more likely embeddable are prioritized for embedding. In other words, the entropy should increase as more of the less likely embeddable blocks are used for embedding if the block sorting algorithm is well designed.

Figure 9 shows the average prediction error entropy of 1000 images from Alaska image data set. Each point is measured for every 10 percentage of the total blocks are used for embedding. From the figure, it is very clear that the entropy is smoothly increasing as a greater number of blocks are used for embedding for both methods. Furthermore, the proposed method has much lower average entropy than the Huang et al.'s (DPCM prediction error histogram).

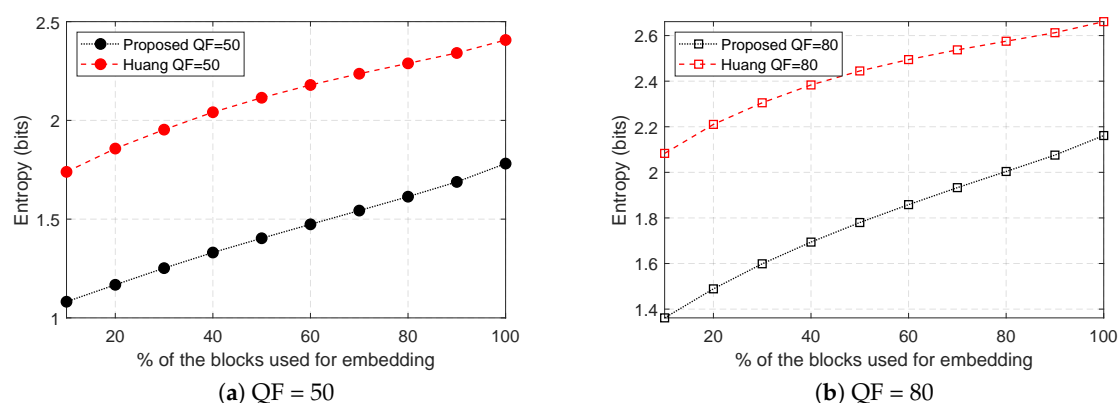


Figure 9. Average prediction error entropy.

8. Conclusions

Reversible data hiding in JPEG image is becoming an important and highly researched topic. With existing work mostly focusing on embedding only using the quantized AC coefficients, there are no good embedding method only using DC (quantized DC coefficients). This is a problem for data analytic applications where AC (quantized AC coefficients) are used for feature extraction for fine details. The proposed method proposes a novel reversible data hiding in DC. It divides the JPEG blocks into two non-overlapping sets and an accurate predictor is proposed, which uses the four neighboring blocks and the ACs. The experimental results show that the proposed method performs better than the existing work.

Author Contributions: Conceptualization, S.K., F.H., H.J.K.; Methodology, S.K.; Software, S.K.; Validation, F.H., and H.J.K.; Formal Analysis, S.K.; Investigation, S.K.; Resources, H.J.K.; Data Curation, S.K., F.H., H.J.K.; Writing—Original Draft Preparation, S.K.; Writing—Review and Editing, S.K., F.H., H.J.K.; Visualization, S.K.; Supervision, F.H., H.J.K.; Project Administration, S.K.; Funding Acquisition, S.K., F.H., H.J.K.

Funding: This work was in part supported by the National Research Foundation of Korea(NRF) grant funded by the Korea government(MEST) (No.NRF-2019R1I1A1A01059582), and in part supported under the framework of international cooperation program managed by the National Research Foundation of Korea(2018K2A9A2A06024168, FY2019)

Conflicts of Interest: The authors declare no conflict of interest.

Abbreviations

The following abbreviations are used in this manuscript:

DCT	Discrete Cosine Transformation
DCT	(Bold font) Quantized DCT coefficients
DC	(Bold font) Quantized DC coefficient
AC	(Bold font) Quantized AC coefficients
PSNR	Peak signal-to-noise ratio
DPCM	JPEG Differential pulse code modulation
QF	Quantization factor

References

1. Liu, Z.; Xu, L.; Guo, Q.; Lin, C.; Liu, S. Image watermarking by using phase retrieval algorithm in gyrator transform domain. *Opt. Commun.* **2010**, *283*, 4923–4927. [\[CrossRef\]](#)
2. Fridrich, J.; Goljan, M.; Du, R. Lossless data embedding-new paradigm in digital watermarking. *EURASIP J. Adv. Signal Process.* **2002**, *2002*, 986842. [\[CrossRef\]](#)
3. Celik, M.U.; Sharma, G.; Tekalp, A.M.; Saber, E. Lossless generalized-LSB data embedding. *IEEE Trans. Image Process.* **2005**, *14*, 253–266. [\[CrossRef\]](#) [\[PubMed\]](#)

4. Celik, M.U.; Sharma, G.; Tekalp, A.M. Lossless watermarking for image authentication: A new framework and an implementation. *IEEE Trans. Image Process.* **2006**, *15*, 1042–1049. [[CrossRef](#)] [[PubMed](#)]
5. Fridrich, J.; Goljan, M.; Du, R. Invertible authentication. In *Security and Watermarking of Multimedia Contents III*; International Society for Optics and Photonics(SPIE): Bellingham, WA, USA, 2001; Volume 4314, pp. 197–208.
6. Xuan, G.; Zhu, J.; Chen, J.; Shi, Y.Q.; Ni, Z.; Su, W. Distortionless data hiding based on integer wavelet transform. *Electron. Lett.* **2002**, *38*, 1646–1648. [[CrossRef](#)]
7. Hwang, H.J.; Kim, H.J.; Sachnev, V.; Joo, S.H. Reversible watermarking method using optimal histogram pair shifting based on prediction and sorting. *KSII Trans. Internet Inf. Syst.* **2010**, *4*, 655–670. [[CrossRef](#)]
8. Tian, J. Reversible data embedding using a difference expansion. *IEEE Trans. Circuits Syst. Video Technol.* **2003**, *13*, 890–896. [[CrossRef](#)]
9. Alattar, A.M. Reversible watermark using the difference expansion of a generalized integer transform. *IEEE Trans. Image Process.* **2004**, *13*, 1147–1156. [[CrossRef](#)]
10. Kamstra, L.; Heijmans, H.J. Reversible data embedding into images using wavelet techniques and sorting. *IEEE Trans. Image Process.* **2005**, *14*, 2082–2090. [[CrossRef](#)]
11. Kim, H.J.; Sachnev, V.; Shi, Y.Q.; Nam, J.; Choo, H.G. A novel difference expansion transform for reversible data embedding. *IEEE Trans. Inf. Forensic Secur.* **2008**, *3*, 456–465.
12. Dragoi, I.C.; Coltuc, D. Adaptive Pairing Reversible Watermarking. *IEEE Trans. Image Process.* **2016**, *25*, 2420–2422. [[CrossRef](#)] [[PubMed](#)]
13. Tai, W.L.; Yeh, C.M.; Chang, C.C. Reversible data hiding based on histogram modification of pixel differences. *IEEE Trans. Circuits Syst. Video Technol.* **2009**, *19*, 906–910.
14. Kim, S.; Qu, X.; Sachnev, V.; Kim, H.J. Skewed Histogram Shifting for Reversible Data Hiding using a Pair of Extreme Predictions. *IEEE Trans. Circuits Syst. Video Technol.* **2018**. [[CrossRef](#)]
15. Coatrieux, G.; Pan, W.; Cuppens-Boulahia, N.; Cuppens, F.; Roux, C. Reversible watermarking based on invariant image classification and dynamic histogram shifting. *IEEE Trans. Inf. Forensic Secur.* **2013**, *8*, 111–120. [[CrossRef](#)]
16. Ni, Z.; Shi, Y.Q.; Ansari, N.; Su, W. Reversible data hiding. *IEEE Trans. Circuits Syst. Video Technol.* **2006**, *16*, 354–362.
17. Lee, S.K.; Suh, Y.H.; Ho, Y.S. Reversible Image Authentication Based on Watermarking. In Proceedings of the IEEE International Conference on Multimedia and Expo, Toronto, ON, Canada, 9–12 July 2006; IEEE: Piscataway, NJ, USA, 2006; pp. 1321–1324.
18. Hwang, J.; Kim, J.; Choi, J. A reversible watermarking based on histogram shifting. *Lect. Notes Comput. Sci.* **2006**, *4283*, 348–361.
19. Ou, B.; Li, X.; Zhao, Y.; Ni, R.; Shi, Y.Q. Pairwise Prediction-Error Expansion for Efficient Reversible Data Hiding. *IEEE Trans. Image Process.* **2013**, *22*, 5010–5021. [[CrossRef](#)]
20. Li, X.; Zhang, W.; Gui, X.; Yang, B. A Novel Reversible Data Hiding Scheme Based on Two-Dimensional Difference-Histogram Modification. *IEEE Trans. Inf. Forensic Secur.* **2013**, *8*, 1091–1100.
21. Ou, B.; Li, X.; Zhao, Y.; Ni, R. Reversible data hiding using invariant pixel-value-ordering and prediction-error expansion. *Signal Process. Image Commun.* **2014**, *29*, 760–772. [[CrossRef](#)]
22. Li, X.; Li, J.; Li, B.; Yang, B. High-fidelity reversible data hiding scheme based on pixel-value-ordering and prediction-error expansion. *Signal Process.* **2013**, *93*, 198–205. [[CrossRef](#)]
23. Peng, F.; Li, X.; Yang, B. Improved PVO-based reversible data hiding. *Digit. Signal Prog.* **2014**, *25*, 255–265. [[CrossRef](#)]
24. Qu, X.; Kim, H.J. Pixel-based pixel value ordering predictor for high-fidelity reversible data hiding. *Signal Process.* **2015**, *111*, 249–260. [[CrossRef](#)]
25. Thodi, D.M.; Rodríguez, J.J. Expansion embedding techniques for reversible watermarking. *IEEE Trans. Image Process.* **2007**, *16*, 721–730. [[CrossRef](#)]
26. Fallahpour, M. Reversible image data hiding based on gradient adjusted prediction. *IEICE Electron. Express* **2008**, *5*, 870–876. [[CrossRef](#)]
27. Sachnev, V.; Kim, H.J.; Nam, J.; Suresh, S.; Shi, Y.Q. Reversible watermarking algorithm using sorting and prediction. *IEEE Trans. Circuits Syst. Video Technol.* **2009**, *19*, 989–999. [[CrossRef](#)]
28. Hong, W.; Chen, T.S.; Shiu, C.W. Reversible data hiding for high quality images using modification of prediction errors. *J. Syst. Softw.* **2009**, *82*, 1833–1842. [[CrossRef](#)]

29. Luo, L.; Chen, Z.; Chen, M.; Zeng, X.; Xiong, Z. Reversible image watermarking using interpolation technique. *IEEE Trans. Inf. Forensic Secur.* **2010**, *5*, 187–193.
30. Hong, W. An efficient prediction-and-shifting embedding technique for high quality reversible data hiding. *EURASIP J. Adv. Signal Process.* **2010**, *2010*, 4:1–4:12. [[CrossRef](#)]
31. Xuan, G.; Shi, Y.Q.; Teng, J.; Tong, X.; Chai, P. Double-Threshold Reversible Data Hiding. In Proceedings of the IEEE International Symposium on Circuits and Systems, Paris, France, 30 May–2 June 2010; IEEE: Piscataway, NJ, USA, 2010; pp. 1129–1132.
32. Gao, X.; An, L.; Yuan, Y.; Tao, D.; Li, X. Lossless data embedding using generalized statistical quantity histogram. *IEEE Trans. Circuits Syst. Video Technol.* **2011**, *21*, 1061–1070.
33. Li, X.; Yang, B.; Zeng, T. Efficient reversible watermarking based on adaptive prediction-error expansion and pixel selection. *IEEE Trans. Image Process.* **2011**, *20*, 3524–3533.
34. Coltuc, D. Improved embedding for prediction-based reversible watermarking. *IEEE Trans. Inf. Forensic Secur.* **2011**, *6*, 873–882. [[CrossRef](#)]
35. Dragoi, C.; Coltuc, D. Improved rhombus interpolation for reversible watermarking by difference expansion. In Proceedings of the 20th European Signal Processing Conference (EUSIPCO), Bucharest, Romania, 27–31 August 2012; IEEE: Piscataway, NJ, USA, 2012; pp. 1688–1692.
36. Wu, H.T.; Huang, J. Reversible image watermarking on prediction errors by efficient histogram modification. *Signal Process.* **2012**, *92*, 3000–3009. [[CrossRef](#)]
37. Qin, C.; Chang, C.C.; Huang, Y.H.; Liao, L.T. An inpainting-assisted reversible steganographic scheme using a histogram shifting mechanism. *IEEE Trans. Circuits Syst. Video Technol.* **2013**, *23*, 1109–1118. [[CrossRef](#)]
38. Coltuc, D.; Dragoi, I.C. Context embedding for raster-scan rhombus based reversible watermarking. In Proceedings of the ACM Workshop on Information Hiding and Multimedia Security, Montpellier, France, 17–19 Junly 2013; pp. 215–220.
39. Dragoi, I.C.; Coltuc, D. Local-Prediction-Based Difference Expansion Reversible Watermarking. *IEEE Trans. Image Process.* **2014**, *23*, 1779–1790. [[CrossRef](#)]
40. Qin, J.; Huang, F. Reversible Data Hiding Based on Multiple Two-Dimensional Histograms Modification. *IEEE Signal Process. Lett.* **2019**, *26*, 843–847. doi:10.1109/LSP.2019.2909080. [[CrossRef](#)]
41. Kim, S.; Lussi, R.; Qu, X.; Kim, H.J. Automatic contrast enhancement using reversible data hiding. In Proceedings of the 2015 IEEE International Workshop on Information Forensics and Security (WIFS), Rome, Italy, 16–19 November 2015; IEEE: Piscataway, NJ, USA; pp. 1–5.
42. Kim, S.; Lussi, R.; Qu, X.; Huang, F.; Kim, H.J. Reversible Data Hiding with Automatic Brightness Preserving Contrast Enhancement. *IEEE Trans. Circuits Syst. Video Technol.* **2018**. [[CrossRef](#)]
43. Ying, Q.; Qian, Z.; Zhang, X.; Ye, D. Reversible Data Hiding With Image Enhancement Using Histogram Shifting. *IEEE Access* **2019**, *7*, 46506–46521. [[CrossRef](#)]
44. Wu, H.T.; Tang, S.; Shi, Y.Q. Image Quality Assessment in Reversible Data Hiding with Contrast Enhancement. In Proceedings of the International Workshop on Digital Watermarking, Magdeburg, Germany, 23–25 August 2017; Springer: Cham, Switzerland, 2017; pp. 290–302.
45. Wu, H.T.; Dugelay, J.L.; Shi, Y.Q. Reversible image data hiding with contrast enhancement. *IEEE Signal Process. Lett.* **2015**, *22*, 81–85. [[CrossRef](#)]
46. Gao, G.; Shi, Y.Q. Reversible Data Hiding Using Controlled Contrast Enhancement and Integer Wavelet Transform. *IEEE Signal Process. Lett.* **2015**, *22*, 2078–2082. [[CrossRef](#)]
47. Wu, H.T.; Huang, J.; Shi, Y.Q. A reversible data hiding method with contrast enhancement for medical images. *J. Vis. Commun. Image Represent.* **2015**, *31*, 146–153. [[CrossRef](#)]
48. Gu, K.; Zhai, G.; Yang, X.; Zhang, W.; Chen, C.W. Automatic contrast enhancement technology with saliency preservation. *IEEE Trans. Circuits Syst. Video Technol.* **2014**, *25*, 1480–1494.
49. Ballesteros, D.; Peña, J.; Renza, D. A Novel Image Encryption Scheme Based on Collatz Conjecture. *Entropy* **2018**, *20*, 901. [[CrossRef](#)]
50. Huang, X.; Ye, G. An Image Encryption Algorithm Based on Time-Delay and Random Insertion. *Entropy* **2018**, *20*, 974. [[CrossRef](#)]
51. Fridrich, J.; Goljan, M.; Du, R. Lossless data embedding for all image formats. In Proceedings of the Security and Watermarking of Multimedia Contents IV, San Jose, CA, USA, 21–24 January 2002; International Society for Optics and Photonics: Bellingham, WA, USA, 2002; Volume 4675, pp. 572–584.

52. Wang, K.; Lu, Z.M.; Hu, Y.J. A high capacity lossless data hiding scheme for JPEG images. *J. Syst. Softw.* **2013**, *86*, 1965–1975. [CrossRef]
53. Mobasser, B.G.; Berger, R.J.; Marcinak, M.P.; NaikRaikar, Y.J. Data embedding in JPEG bitstream by code mapping. *IEEE Trans. Image Process.* **2009**, *19*, 958–966. [CrossRef]
54. Qian, Z.; Zhang, X. Lossless data hiding in JPEG bitstream. *J. Syst. Softw.* **2012**, *85*, 309–313. [CrossRef]
55. Hu, Y.; Wang, K.; Lu, Z.M. An improved VLC-based lossless data hiding scheme for JPEG images. *J. Syst. Softw.* **2013**, *86*, 2166–2173. [CrossRef]
56. Chang, C.C.; Lin, C.C.; Tseng, C.S.; Tai, W.L. Reversible hiding in DCT-based compressed images. *Inf. Sci.* **2007**, *177*, 2768–2786. [CrossRef]
57. Lin, C.C.; Shiu, P.F. DCT-based reversible data hiding scheme. In Proceedings of the 3rd International Conference on Ubiquitous Information Management and Communication, Suwon, Korea, 15–16 January 2009; ACM: New York, NY, USA, 2009; pp. 327–335.
58. Xuan, G.; Shi, Y.Q.; Ni, Z.; Chai, P.; Cui, X.; Tong, X. Reversible data hiding for JPEG images based on histogram pairs. In Proceedings of the International Conference Image Analysis and Recognition, Montreal, QC, Canada, 22–24 August 2007; Springer: Berlin/Heidelberg, Germany, 2007; pp. 715–727.
59. Sakai, H.; Kuribayashi, M.; Morii, M. Adaptive reversible data hiding for JPEG images. In Proceedings of the 2008 International Symposium on Information Theory and Its Applications, Auckland, New Zealand, 7–10 December 2008; IEEE: Piscataway, NJ, USA, 2008; pp. 1–6.
60. Li, Q.; Wu, Y.; Bao, F. A reversible data hiding scheme for JPEG images. In Proceedings of the Pacific-Rim Conference on Multimedia, Shanghai, China, 21–24 September 2010; Springer: Berlin/Heidelberg, Germany, 2010; pp. 653–664.
61. Efimushkina, T.; Egiazarian, K.; Gabbouj, M. Rate-distortion based reversible watermarking for JPEG images with quality factors selection. In Proceedings of the European Workshop on Visual Information Processing (EUVIP), Tampere, Finland, 26–28 November 2018; IEEE: Piscataway, NJ, USA, 2013; pp. 94–99.
62. Huang, F.; Qu, X.; Kim, H.J.; Huang, J. Reversible data hiding in JPEG images. *IEEE Trans. Circuits Syst. Video Technol.* **2015**, *26*, 1610–1621. [CrossRef]
63. Hou, D.; Wang, H.; Zhang, W.; Yu, N. Reversible data hiding in JPEG image based on DCT frequency and block selection. *Signal Process.* **2018**, *148*, 41–47. [CrossRef]
64. Wedaj, F.T.; Kim, S.; Kim, H.J.; Huang, F. Improved reversible data hiding in JPEG images based on new coefficient selection strategy. *EURASIP J. Image Video Process.* **2017**, *2017*, 63. [CrossRef]
65. Information Technology-Digital Compression and Coding of Continuous-Tone Still Images: Requirements and Guidelines, Document T.81, 1992. Available online: <https://www.w3.org/Graphics/JPEG/itu-t81.pdf> (accessed on 23 August 2019).
66. Wang, J.; Ni, J. A GA optimization approach to HS based multiple reversible data hiding. In the Proceedings of the IEEE International Workshop on Information Forensics and Security, Guangzhou, China, 3–6 December 2013; pp. 203–208.



© 2019 by the authors. Licensee MDPI, Basel, Switzerland. This article is an open access article distributed under the terms and conditions of the Creative Commons Attribution (CC BY) license (<http://creativecommons.org/licenses/by/4.0/>).